JPET Fast Forward. Published on February 22, 2013 as DOI: 10.1124/jpet.112.201442
JPET Fast Forward. Published on February 22, 2013 as DOI: 10.1124/jpet.112.201442
This article has not been copyedited and formatted. The final version may differ from this version.

Attenuation by Statins of Membrane Raft-Redox Signaling in Coronary Arterial Endothelium

Yu-Miao Wei, Xiang Li, Jing Xiong, Justine M. Abais, Min Xia, Krishna M. Boini, Yang Zhang, Pin-Lan Li

Department of Pharmacology & Toxicology, Medical College of Virginia Campus, Virginia Commonwealth University, Richmond, Virginia (Y.-M.W., X.L., J.X., J.-M.A., M.X., K.-M.B., Y.Z., P.-L.L.)

Downloaded from jpet.aspetjournals.org at ASPET Journals on April 9, 2024

Copyright 2013 by the American Society for Pharmacology and Experimental Therapeutics.

JPET Fast Forward. Published on February 22, 2013 as DOI: 10.1124/jpet.112.201442
This article has not been copyedited and formatted. The final version may differ from this version.

Running title: Statins inhibit NADPH oxidase associated with membrane rafts

Correspondence should be addressed to:

Yang Zhang, Department of Pharmacology & Toxicology, Medical College of Virginia Campus, Virginia Commonwealth University, Richmond, VA 23298

Tel: (804) 828-0738, Fax: (804) 828-4794, E-mail: yzhang3@vcu.edu

Number of text pages: 26

Number of tables: 0

Number of figures: 8

Number of reference: 49

Number of words in the Abstract: 250

Number of words in Introduction: 873

Number of words in Discussion: 1655

List of abbreviations:

Acid sphingomyelinase (ASM); CMH: 1-hydroxy-3-methoxycarbonyl-2,2,5,5-tetramethylpyrorolidine; CTXB, cholera toxin B; DHE, Dihydroethidium; eNOS, endothelial nitric oxide synthase; ESR, electronic spin resonance; HCAEC: human coronary endothelial cell; LOX-1, lectin-like oxidized low-density lipoprotein, MCD, methyl-β-cyclodextrin; MR, membrane raft; NO, nitric oxide; OxLDL, oxidized low-density lipoprotein; TR, Texas Red;

Section: Cardiovascular

Downloaded from jpet.aspetjournals.org at ASPET Journals on April 9, 2024

JPET Fast Forward. Published on February 22, 2013 as DOI: 10.1124/jpet.112.201442
This article has not been copyedited and formatted. The final version may differ from this version.

ABSTRACT

Membrane raft (MR)-redox signaling platforms associated with NADPH oxidase are involved in coronary endothelial dysfunction. Here, we studied whether statins interfere with the formation of MR-redox signaling platforms to protect the coronary arterial endothelium from oxidized low-density lipoprotein (OxLDL)-induced injury and from acute hypercholesterolemia. In cultured human coronary arterial endothelial cells (HCAECs), confocal microscopy detected the formation of a MRs clustering when they were exposed to OxLDL, and such MR platform formation was inhibited markedly by statins including pravastatin and simvastatin. In these MR clusters, NADPH oxidase subunits, $gp91^{phox}$ and $p47^{phox}$ were aggregated, which was markedly blocked by both statins. Besides that, co-localization of acid sphingomyelinase (ASM) and ceramide was induced by OxLDL, which was blocked by statins. Electron spin resonance spectrometry showed that OxLDL-induced superoxide ($O_2^{\cdot -}$) production in the MR fractions was substantially reduced by statins. In coronary artery intima of mice with acute hypercholesterolemia, confocal microscopy demonstrated a co-localization of $gp91^{phox}$, $p47^{phox}$, ASM or ceramide within MR clusters. Such co-localization was rarely observed in the arteries of normal mice or significantly reduced by pretreatment of hypercholesterolemic mice with statins. Further, $O_2^{\cdot -}$ production *in situ* was 3 folds higher in the coronary arteries from hypercholesterolemic mice than normal mice, and such increase was inhibited by statins. Our results indicate that blockade of MR redox signaling platform formation in endothelial cell membrane may be another important therapeutic mechanism of statins in preventing endothelial injury and atherosclerosis, which may be associated with their direct action on membrane cholesterol structure and function.

Downloaded from jpet.aspetjournals.org at ASPET Journals on April 9, 2024

JPET Fast Forward. Published on February 22, 2013 as DOI: 10.1124/jpet.112.201442
This article has not been copyedited and formatted. The final version may differ from this version.

INTRODUCTION

Statins, inhibitors of 3-hydroxy-3-methylglutaryl coenzyme A (HMG-CoA) reductase, are widely used to lower plasma cholesterol and treat atherosclerotic diseases (Greenwood and Mason, 2007; Wang et al., 2008; Libby et al., 2009). Since approximately 60-70% of serum cholesterol is derived from *de novo* cholesterol synthesis in the liver, inhibition of HMG-CoA reductase is able to inhibit mevalonate pathway to block cholesterol biosynthesis and thereby result in a dramatic reduction in circulating low-density lipoprotein (LDL)-cholesterol (1994; 1998). Thus, lowering serum cholesterol levels is thought to be the primary mechanism underlying the therapeutic benefits of statins' therapy in atherosclerosis and related cardiovascular diseases. In addition to their cholesterol-lowering effect, statins exhibit non-cholesterol-lowering activity to inhibit inflammatory responses of immune cells including macrophages and lymphocytes, which has been associated with inhibition of mevalonate pathway to block the synthesis of isoprenoid intermediates such as farnesyl pyrophosphate (FPP) and geranylgeranyl pyrophosphate (GGPP) and prevent protein prenylation and consequent membrane trafficking of small G proteins such as Rho, Ras, and Rac (Bu et al., 2011). Previous studies have demonstrated that both cholesterol-lowering and non-cholesterol-lowering action may contribute to the beneficial effects of statins in protecting endothelial function in endothelial cells (ECs) via inhibiting NADPH oxidase-mediated redox signaling (Mason et al., 2004; Tawfik et al., 2006; Jacobson, 2009). First, statins lower the cholesterol level in ECs resulting in augmentation of endothelial nitric oxide synthase (eNOS) activation and suppression of superoxide ($O_2^{\cdot -}$) production (Mason et al., 2004; Tawfik et al., 2006; Jacobson, 2009). Under resting condition, eNOS activity is inhibited by binding to a membrane caveolar protein called cavolin-1. By interfering with cholesterol biosynthesis and lowering plasma membrane cholesterol levels, statins were shown to decrease the expression of caveolin-1 resulting in eNOS activation and nitric oxide (NO) production (Mason et al., 2004). Second, by preventing isoprenylation of Rac1, which is important for NADPH oxidase activation, recent studies have demonstrated that statins inhibit $O_2^{\cdot -}$ formation in ECs upon stimulation of injury factors or under pathological conditions such as angiotensin II, homocysteine, hyperglycemia (Wagner et al., 2000; Vecchione et al., 2007; Briones et al., 2009; Alvarez et al., 2010; Bao et al., 2010c). However, it remains unknown how statins alter the assembling and aggregation of NADPH oxidase subunits and thereby affect its activity to produce $O_2^{\cdot -}$ in addition to their effect on Rac1 or eNOS.

Downloaded from jpet.aspetjournals.org at ASPET Journals on April 9, 2024

JPET Fast Forward. Published on February 22, 2013 as DOI: 10.1124/jpet.112.201442
This article has not been copyedited and formatted. The final version may differ from this version.

Recent studies have indicated that membrane rafts (MRs, formerly lipid rafts) are of importance in mediating and amplifying a variety of cellular signals (Zhang et al., 2009), which may be a target for the action of statins. MRs are dynamic assemblies of cholesterol, lipids with saturated acyl chains, such as sphingolipids and glycosphingolipids, in the exoplasmic leaflet of the membrane bilayer, and cholesterol in the inner leaflet. MRs clustering is emerging as a novel mechanism mediating the transmembrane signaling in response to various stimuli in a variety of cell types, including lymphocytes, endothelial cells, and neurons (Zhang et al., 2009). Clustered MRs form membrane signaling platforms, in particular, the ceramide-enriched platforms or macrodomains (Zhang et al., 2009). These membrane platforms can recruit or aggregate various signaling molecules such as small G proteins, tyrosine kinases, and phosphatases, resulting in the activation of different signaling pathways. More recently, there are increasing evidences that MRs clustering on the arterial ECs is an important initiating mechanism in endothelial injury in response to damaging factors such as death receptor agonists, inflammatory factors, irradiation (Natoli et al., 1998; Zhang et al., 2006; Zhang et al., 2009). It has been shown that MRs clustering recruits or aggregates redox signaling molecules such as NADPH oxidase subunits, $gp91^{phox}$, $p47^{phox}$, and Rac GTPase, resulting in the formation of a membrane signal amplification platform that activates and enhance production of $O_2^{\cdot -}$ (Zhang et al., 2006; Zhang et al., 2007). These MR signaling platforms associated with $O_2^{\cdot -}$ production have been referred as MR redox signaling platforms. The formation of such MR redox signaling platforms in the EC membrane is associated with ceramide production via lysosomal acid sphingomylinase (ASM), which is translocated onto the plasma membrane via membrane proximal lysosome trafficking and fusion upon stimulation of death receptors (Jin et al., 2008a; Bao et al., 2010a; Bao et al., 2010b). It has been shown that this lysosomal ASM-mediated formation of redox signaling platforms could be inhibited by cholesterol depletion reagents, methyl-β-cyclodextrin and filipin (Zhang et al., 2006; Zhang et al., 2007). Statins has been shown to decreases plasma membrane cholesterol in ECs (Mason et al., 2004). In this regard, it is plausible that statins may interfere with the MR redox signaling via their cholesterol-lowering action and thus prevent endothelial dysfunction in coronary arteries.

In this study, we first determined whether statins inhibit the formation of MR-redox signaling

Downloaded from jpet.aspetjournals.org at ASPET Journals on April 9, 2024

JPET Fast Forward. Published on February 22, 2013 as DOI: 10.1124/jpet.112.201442
This article has not been copyedited and formatted. The final version may differ from this version.

platforms to decrease $O_2^{\cdot -}$ production in ECs stimulated by a proatherogenic factor, oxidized low-density lipoprotein (OxLDL). Then, we extended our studies to animal experiments to test whether this action of statins on MR clustering can be observed. Using a typical mouse model of acute hypercholesterolemia, we determined the effects of statins treatment on MR clustering, NADPH oxidase assembly and $O_2^{\cdot -}$ production in the coronary arterial. Our results indicate that blockade of MR redox signaling platform formation in EC membrane is another important therapeutic mechanism of statins in preventing ROS formation during endothelial injury and atherosclerosis.

MATERIALS AND METHODS

Cell culture and stimulation

Human coronary arterial endothelial cells (HCAECs) were purchased and maintained in commercially available endothelial cell growth medium (Invitrogen, CA) as we described previously [39]. All studies were performed by using HCAECs of 3 to 5 passages. OxLDL (KALEN Human Medium OxLDL^{TM}) was used as proatherogenic stimuli to treat HCAECs. Pravastatin and simvastatin (both statins were purchased from Sigma) were selected as prototype statins to treat cells and mice because pravastatin is typical water-soluble statin while simvastatin is typical lipid-soluble one. Cells were pretreated with pravastatin (10 μM) or simvastatin (5 μM) for 1 hour and then stimulated with OxLDL (100 μg/mL) for 15 min in all experiments of the present study if not otherwise mentioned. Simvastatin was activated by opening the lactone ring by dissolving in 95% ethanol and 0.1 N NaOH, heating at 50 ^{o}C for 2 h, and neutralizing with HCl to pH 7.2 as described previously (Gerson et al., 1989; Tawfik et al., 2006). The dosages of statins were chosen based on previous studies (Dje N'Guessan et al., 2009; Alvarez et al., 2010) and our observations that statins at these doses did not significantly induced morphological signs of cytotoxicity in HCAECs. Some groups of cells were pretreated with mevalonate (Mev, 10 μM), farnesol (Far, 10 μM), geranylgeraniol (Ger, 10 μM), methyl-β-cyclodextrin (MCD, 1 mM) or filipin (1 μg/ml) (all reagents were purchased from Sigma) for 1 hour. Plasmids containing cDNA encoding oncogenic *Rac1* gene were used as we previously described (Yi et al., 2009). Transfection of cDNA plasmids was performed using the TransFectin Lipid Reagent (Bio-Rad, CA, USA) according to the manufacturer's instructions.

Downloaded from jpet.aspetjournals.org at ASPET Journals on April 9, 2024

JPET Fast Forward. Published on February 22, 2013 as DOI: 10.1124/jpet.112.201442
This article has not been copyedited and formatted. The final version may differ from this version.

Confocal microscopy of MRs and related proteins in HCAECs

For confocal detection of MR platforms or MR-associated proteins, HCAECs were grown on poly-L-lysine coated chamber slides, stimulated or remain unstimulated, fixed in PFA/PBS for 10 min. Detection of MR clusters was performed as we described previously (Jin et al., 2008a). In brief, cells were fixed, unpermeablized and stained with Alexa Fluor 488-conjugated cholera toxin B (Al488-CTXB, 2 μg/mL) (Molecular Probes, OR), which specifically binds to G_{M1} gangliosides enriched in MRs. The patch formation of Al488-CTXB labeled gangliosides complex represented the MR clusters. Clustering was defined as one or several intense spots of fluorescence on the cell surface, whereas unstimulated cells showed a homogenous distribution of fluorescence throughout the membrane. In each experiment, the presence or absence of clustering in samples of 200 cells was scored by two independent observers after specifying the criteria for positive spots of fluorescence. Cells displaying a homogeneous distribution of fluorescence were marked negative. Results were given as the percentage of cells showing one or more clusters after the indicated treatment as described.

To detect the co-localization of ASM with ceramide in HCAECs, the cells were incubated with rabbit anti-ASM (1:200, Santa Cruz Biotechnology) and mouse anti-ceramide antibodies (1:200, Alexis Biochemicals). Then cells were stained for another hour with Alexa Fluor 488 (Al488)-labeled donkey anti-rabbit and Texas Red (TR)-labeled donkey anti-mouse antibodies (1:500, Invitrogen). Similarly, for detection of the co-localization of MRs with $gp91^{phox}$ or $p47^{phox}$, HCAECs were first incubated with Al488-CTXB (2 μg/mL) and mouse monoclonal anti-$gp91^{phox}$ or anti-$p47^{phox}$ (1:200, BD Biosciences) followed by incubation with Texas Red-conjugated anti-mouse (1:500, Invitrogen). Then, the slides were washed, mounted, and visualized through sequentially scanning on an Olympus laser scanning confocal microscope (Fluoview FV1000, Olympus, Japan). Colocalization was analyzed by Image Pro Plus software, and the colocalization coefficient was represented by Pearson's correlation coefficient. All antibodies and probes were incubated at room temperature for one hour if not mentioned.

Electronic spin resonance spectrometric detection of $O_2^{\cdot-}$

Downloaded from jpet.aspetjournals.org at ASPET Journals on April 9, 2024

JPET Fast Forward. Published on February 22, 2013 as DOI: 10.1124/jpet.112.201442
This article has not been copyedited and formatted. The final version may differ from this version.

Electronic spin resonance (ESR) detection of $O_2^{\cdot-}$ was performed as we described previously (Zhang et al., 2007). In brief, HCAECs were gently collected and suspended in modified Krebs-HEPES buffer containing deferoxamine (100 μM, metal chealtor). Approximately 1×10^6 HCAECs were incubated with OxLDL (100 μg/mL) or bacterial sphingomyelinase (0.01 U/mL, Sigma) for 30 min in the absence or presence of statins (pravastatin 10 μM; simvastatin 5 μM), then mixed with 1 mM spin trap 1-hydroxy-3-methoxycarbonyl- 2,2,5,5-tetramethylpyrorolidine (CMH) (Noxygen, Elzach, Germany) in the presence or absence of 100 units/ml polyethylene glycol (PEG)-conjugated superoxide dismutase (SOD). The cell mixture loaded in glass capillaries was immediately analyzed for $O_2^{\cdot-}$ production at each minute for 10 min using a Miniscope MS200 ESR spectrometer (Magnettech, Germany). The ESR settings were as follows: biofield, 3350; field sweep, 60G; microwave frequency, 9.78 GHz; microwave power, 20 mW; modulation amplitude, 3G; 4096 points of resolution; receiver gain, 100; and kinetic time, 10 min. The SOD-inhibitable signals were normalized by protein concentration and compared among different experimental groups.

Acute hypercholesterolemia in mice

Poloxamer 407 (P407) (Sigma-Aldrich) was used to induce acute hypercholesterolemia in mice as described previously (Johnston et al., 2006). In brief, twenty 6-week old C57BL/6 mice (The Jackson Laboratory, Bar Harbor, ME) were randomly divided into 4 groups: control group, P407 group (hypercholesterolemia) group, statin group, and P407 plus statin group with 5 mice for each group. The mice from statin group and P407 plus statin group were intragastric fed statins (pravastatin 140 mg/kg/d; simvastatin 70 mg/kg/d) for a week, the other mice were fed tap water. The dosage for statins was in agreement with previous studies in which simvastatin or pravastatin administered to the mice was either lower or higher (Bea et al., 2002; Araki et al., 2008; Sharyo et al., 2008). On the day of the P407 administration, mice from P407 group or P407 plus statin group were intraperitoneally injected with P407 (0.5 g/kg), while mice from control group and statin group were administrated with the same volume of sterile saline. 24 hours after P-407 or normal saline treatment, blood samples of mice were obtained by periorbital sampling when mice were under ether anesthesia. Then, the plasma samples were isolated by centrifugation and frozen at -80°C until analysis. After blood collection, the animals under ether anesthesia were sacrificed by cervical dislocation. The hearts with coronary artery were obtained and frozen in liquid nitrogen for the preparation of frozen section

Downloaded from jpet.aspetjournals.org at ASPET Journals on April 9, 2024

JPET Fast Forward. Published on February 22, 2013 as DOI: 10.1124/jpet.112.201442
This article has not been copyedited and formatted. The final version may differ from this version.

slides. All protocols were approved by the Institutional Animal Care and Use Committee of the Virginia Commonwealth University. All animals were provided standard rodent chow and water ad libitum in a temperature-controlled room.

Assay of the cholesterol levels in the plasma of mice

The cholesterol concentrations in mouse plasma were determined using a standard fluorescence assay kit (EnzyChrom AF Cholesterol Assay Kit) as described previously (Johnston et al., 2006). Cholesterol is oxidized to yield hydrogen peroxide in a reaction catalyzed by cholesterol oxidase. In the presence of horseradish perioxidase, hydrogen peroxide is able to oxidize none-fluorescent 10-acetyl-3,7-dihydroxyphenoxazine into highly fluorescent resorufin. The fluorescent intensity was determined at excitation/emission of 485/530 nm using fluorescent microplate reader (FLx800, BIO-TEK Instruments) and used to calculate cholesterol concentrations following manufacturer's instruction.

Confocal microscopy of MRs and related proteins in coronary arterial intima of mice

The MR clusters and NADPH oxidase subunits in the coronary arterial intima were detected as described previously with some modifications (Jankov et al., 2005)[34]. Briefly, the mouse hearts were frozen in Tissue-Tek OCT and cut by cryostat into 10 μm sections and mounted on Superfrost/Plus slides. After fixation with acetone, the frozen section slides were incubated with rabbit anti-flotillin-1 antibody (1:50, Cell Signaling) and mouse anti-gp91^{phox} or anti-p47^{phox} antibody overnight at 4°C (BD Biosciences). Similarly, detection of the co-localization of MR clusters with ASM or ceramide was performed by incubating section slides with same rabbit anti-flotillin-1 as above and mouse anti-ceramide (BD Biosciences) antibodies or with a mouse anti-flotillin-1 (BD Biosciences) and rabbit anti-ASM antibodies (Santa Cruz Biotechnology). After incubation with primary antibodies, the slides were washed and labeled with corresponding Alexa Fluor-488 and Alexa Fluor-555 conjugated secondary antibodies (Invitrogen). All primary antibodies were used at a dilution of 1:50 and all secondary antibodies were used at a dilution of 1:200. Then, the slides were washed, mounted, and subjected to confocal microscopic analysis (Fluoview FV1000, Olympus, Japan).

Downloaded from jpet.aspetjournals.org at ASPET Journals on April 9, 2024

JPET Fast Forward. Published on February 22, 2013 as DOI: 10.1124/jpet.112.201442
This article has not been copyedited and formatted. The final version may differ from this version.

In situ detection of $O_2^{\cdot-}$ production in mouse coronary arteries

Dihydroethidium (DHE) is a lipophilic cell-permeable dye that can be oxidized by $O_2^{\cdot-}$ to form ethidium bromide. Ethidium then binds irreversibly to the double-stranded DNA (such as chromosomal DNA) causing amplification of a red fluorescent signal at 480/610 nm excitation-emission. The $O_2^{\cdot-}$ produced in the arterial wall was detected *in situ* by using DHE as probes (Molecular Probes, OR) as described previously (Jankov et al., 2008; Nijmeh et al., 2010). Briefly, the unfixed tissue slides from different groups were incubated with DHE (10 μM) in PBS at room temperature for 30 min. Then, the slides were washed, fixed, mounted, and subjected to confocal microscopic analysis (Fluoview FV1000, Olympus, Japan). In some experiments, the tissue slides were incubated at room temperature for 30 min in the presence of NADPH oxidase specific inhibitor gp91 ds-tat peptide (ANASPEC Inc., 5 μM) or $O_2^{\cdot-}$ scavenger PEG-SOD (Sigma, 100 U/ml).

Statistics analysis

Data are presented as means ± SEM. Significant differences between and within multiple groups were examined using one-way ANOVA test for followed by Duncan's multiple-range test. A Students' *t* test was used to detect significant difference between two groups. The statistic analysis was performed by SigmaStat 3.5 software (Systat Software, IL). $P<0.05$ was considered statistically significant.

RESULTS

Statins inhibit OxLDL-induced MR clustering in HCAECs.

Figure 1A presents the representative fluorescent confocal microscopic images showing Alexa488-CTXB-labeled patches in the membrane of HCAECs. Under resting conditions (control), there was only a diffuse fluorescent staining in the cell membrane indicating a possibly evenly distributed single MRs. CTXB specifically binds with ganglioside G_{M1} enriched in MRs. When HCAECs were incubated with OxLDL, some large fluorescent dots or patches were observed in the membrane, indicating MRs aggregated on the cell membrane upon OxLDL treatment. In statins (pravastatin and simvastatin)-pretreated groups, the number of green spot or patches was decreased, indicating that the MR clustering is attenuated. Figure 1B summarized the effects of different doses

Downloaded from jpet.aspetjournals.org at ASPET Journals on April 9, 2024

JPET Fast Forward. Published on February 22, 2013 as DOI: 10.1124/jpet.112.201442
This article has not been copyedited and formatted. The final version may differ from this version.

of OxLDL on the MR clustering by counting the percentage of cells with these MR clusters or patches. We found that control cells displayed a small percentage with MR clustering (26.4 ± 5.8%). After these cells were stimulated with OxLDL, MR-clustered positive cells increased significantly with a maximum response of 70.1 ± 6.1% at 100 μg/ml. When these cells were pretreated with pravastatin or simvastatin, OxLDL-induced MR clustering was significantly inhibited. These inhibitory effects of statins could be reversed by treating the cells with mevalonate (Mev) or farnesol (Far) but not with geranylgeraniol (Ger) or by overexpression of oncogenic Rac1 GTPase.

Statins inhibit OxLDL-induced ASM translocation and ceramide production in HCAECs.

Previous studies have shown that lysosomal trafficking and translocation of ASM into MRs result in ceramide production, MR clustering and formation of ceramide-enriched macrodomains (Jin et al., 2008a). To examine whether ASM/ceramide is involved in OxLDL-induced MR clustering and whether OxLDL-induced MR clustering forms ceramide-enriched macrodomains, we stained HCAECs with Alexa488-conjuated anti-ASM and Texas Red-labeled anti-ceramide. As shown in Figure 2A, OxLDL stimulation caused an aggregation of ASM in ceramide-enriched macrodomains, which exhibited as yellow dots or patches. When these cells were pretreated with pravastatin or simvastatin, OxLDL-induced ASM aggregation in ceramide clusters was significantly blocked. This result means that Ox-LDL led to ASM translocation and ceramide production in the cell membrane, especially in MRs domain (see below), which can be blocked by statins. Summarized co-localization coefficiency shown in Figure 2B suggests that statins markedly block OxLDL-induced ASM translocation, ceramide production and subsequent formation of ceramide-enriched macrodomains.

Statins prevent OxLDL-induced NADPH oxidase subunits aggregation in MR clusters.

To examine whether NADPH oxidase subunits are able to aggregate in MR clusters upon OxLDL stimulation, we stained HCAECs with both Al488-CTXB and Texas Red-conjugated anti-gp91^{phox} or anti-p47^{phox} antibodies, and the distribution of gp91 ^{phox} or p47 ^{phox} within MR clusters was visualized by confocal microscopy. As shown in Figure 3A, gp91^{phox}, a membrane associated subunit of NADPH oxidase was evenly distributed throughout the whole cell under control condition and no co-localization of gp91^{phox} within CTXB-positive MR dots or patches was observed. When HCAECs were stimulated with OxLDL, gp91^{phox} was aggregated in MR clusters as shown by strong yellow

Downloaded from jpet.aspetjournals.org at ASPET Journals on April 9, 2024

JPET Fast Forward. Published on February 22, 2013 as DOI: 10.1124/jpet.112.201442
This article has not been copyedited and formatted. The final version may differ from this version.

fluorescent dots or patches. In Figure 3B, $p47^{phox}$, a cytosolic subunit of NADPH oxidase was also found to evenly spread throughout the whole cell mainly in cytosol under control condition. OxLDL induced translocation of $p47^{phox}$ into MR clusters as shown by co-localization of $p47^{phox}$ in CTXB-positive yellow dots or patches. In pravastatin and simvastatin pretreated HCAECs, however, OxLDL-induced aggregation of $gp91^{phox}$ and translocation of $p47^{phox}$ in MR clusters were significantly attenuated (Figure 3A-C). These results indicate that upon OxLDL stimulation MR clusters with recruitment or aggregation of NADPH oxidase subunits formed a number of MR-NADPH oxidase complexes (referred to as MR redox signaling platforms) that possess redox signaling function. Moreover, these effects of OxLDL were inhibited by statins.

Effects of statins on OxLDL-induced $O_2^{\cdot -}$ production in HCAECs

Using electron spin resonance spectrometric (ESR) analysis, we determined the production of $O_2^{\cdot -}$ in HCAECs induced by OxLDL in the absence or presence of statins. Figure 4A depicts representative ESR spectrographs of $O_2^{\cdot -}$ production as trapped by CMH under different treatments. As shown in summarized data in Figure 4B, OxLDL alone increased $O_2^{\cdot -}$ production by 2.7 ± 0.2 folds compared to control. When these cells were pretreated with pravastatin and simvastatin, OxLDL-induced $O_2^{\cdot -}$ production was reduced. Methyl-β-cyclodextrin (MCD) and filipin are potent chemical chelators for cholesterol and used as MR disruptors. Similar to statins, these two MR disruptors inhibited OxLDL-induced $O_2^{\cdot -}$ production. Moreover, sphingomyelinase-induced production of $O_2^{\cdot -}$ could be inhibited by pravastatin and simvastatin as well as methyl-β-cyclodextrin (Figure 4C).

Blockade of P407-induced increase in plasma cholesterol in mice by statins

To determine the inhibitory role of statins on OxLDL-induced NADPH oxidase activation and $O_2^{\cdot -}$ production *in vivo*, we pretreated mice with vehicle or a cocktail of stains and then induced acute hypercholesterolemia by treating mice with P407 for 24 hours. As shown in Figure 5, P407 caused a 9.8-fold increase in plasma cholesterol concentration in control mice, suggesting that these P407-treated mice suffered from acute hypercholesterolemia. In mice treated with statins alone, the basal cholesterol level decreased significantly by 34% compared to control mice. In mice pretreated with statins, P407-induced increase in cholesterol level was reduced by 64% compared to that of vehicle-pretreated mice.

Downloaded from jpet.aspetjournals.org at ASPET Journals on April 9, 2024

JPET Fast Forward. Published on February 22, 2013 as DOI: 10.1124/jpet.112.201442
This article has not been copyedited and formatted. The final version may differ from this version.

Co-localization of gp91^{phox} and p47^{phox} within MRs in arterial intima of hypercholesterolemic mice

To determine whether NADPH oxidase subunits aggregate in MR clusters in the arterial intima exposed to high cholesterol concentration, we stained frozen sections of mouse hearts with the MR marker protein, FITC-conjugated anti-flotillin-1 and Texas Red-conjugated anti-gp91^{phox} or anti-p47^{phox} and then examined the co-localization of flotillin-1 with gp91^{phox} or p47^{phox} in the coronary arteries. As shown in Figure 6A and 6B, typical merged images show strong yellow patches in the edge of arterial lumen in P407-treated mice indicating the co-localization of gp91^{phox} or p47^{phox} within MR clusters in arterial intima. No such yellow patches were observed in the arteries of control mice or mice treated with statins alone. Further, pretreatment of mice with statins significantly reduced the formation of yellow patches in the arterial intima of P407-treated mice. Figure 6C shows summarized co-localization coefficiency in these mice.

Co-localization of ASM or ceramide within MRs in artery intima of hypercholesterolemia mice

As shown in Figure 7, co-localization of ceramide or ASM within MRs was examined in mouse arteries similar to Figure 6. We found no co-localization of either ASM or ceramide within MRs in arteries from control mice, however, strong co-localization of ASM or ceramide was observed (shown as yellow patches) in the edge of arterial lumen from P407-treated mice. Pretreatment of mice with statins abolished such co-localization as yellow fluorescence was markedly reduced. Figure 7C shows summarized co-localization coefficiency between flotillin-1 and ASM or ceramide. These results suggest that acute hypercholesterolemia in mice causes translocation of ASM into MRs and consequent activation of this enzyme resulting in ceramide production, which promotes MRs clustering and formation of ceramide-enriched platforms. This high plasma cholesterol-induced ASM translocation/activation and ceramide production could be blocked by statins.

Statins inhibit O_2^- production in the coronary arterial intima of mice with hypercholesterolemia

To evaluate the ROS production in the arteries of mice with acute hypercholesterolemia and the effect of statin intervention, we stained frozen sections from mouse hearts with dihydroethidium

Downloaded from jpet.aspetjournals.org at ASPET Journals on April 9, 2024

JPET Fast Forward. Published on February 22, 2013 as DOI: 10.1124/jpet.112.201442
This article has not been copyedited and formatted. The final version may differ from this version.

(DHE) and examined *in situ* $O_2^{\cdot -}$ production in the arterial lumen. As shown in Figure 8A, DHE fluorescence (red color) was observed in the arterial walls of control mice indicating a basal level of $O_2^{\cdot -}$ production in the arteries. This DHE-fluorescence was significantly higher in the arteries of P407-treated mice, whereas statins pretreatment (pravastatin and simvastatin) significantly decreased DHE-fluorescence in the arteries of both control and P407-treated mice. The increase in DHE-fluorescence in the arteries from P407-treated mice was also markedly attenuated when the detection was performed in the presence of $O_2^{\cdot -}$ scavenger superoxide dismutase (SOD) or gp91 ds-tat peptide, which is a synthetic peptide (ANASPEC Inc.) that interacts with NADPH oxidase subunit $gp91^{phox}$ and inhibit its activity (data not shown). Therefore, DHE fluorescence signal can be used as an indirect measure for $O_2^{\cdot -}$ production in our experiment settings. Figure 8B summarized the quantitative increases in DHE-fluorescence in the arterial walls of control or hypercholesterolemiac mice without or with statin pretreatment.

Downloaded from jpet.aspetjournals.org at ASPET Journals on April 9, 2024

JPET Fast Forward. Published on February 22, 2013 as DOI: 10.1124/jpet.112.201442
This article has not been copyedited and formatted. The final version may differ from this version.

DISCUSSION

The present study demonstrated that statins inhibit NADPH oxidase assembly and activation in MR-redox signaling platforms in ECs induced by OxLDL and in the coronary arterial endothelium of mice under acute hypercholesterolemia. Our results prove a hypothesis that OxLDL induces the generation of ROS through MRs aggregation and MRs-redox signal platform formation that are mediated by ASM translocation and activation. Statins may improve the endothelial function through blocking this MR signaling pathway by blockade of ASM activation, MRs clustering and MRs-redox platform formation.

OxLDL is a proatherogenic lipoprotein, which leads to vascular dysfunction at the early stage of atherosclerosis. It has been reported that elevated serum levels of OxLDL are associated with increased risk of endothelial dysfunction and coronary artery diseases (Steinberg and Witztum, 2002; Li and Mehta, 2005; Zhu et al., 2005; Heinecke, 2006), where NADPH oxidase activity and $O_2^{\cdot -}$ production were found significantly enhanced (Li and Mehta, 2005; Zhu et al., 2005; Chow et al., 2007). In this regard, accumulating evidence suggest that MRs clustering promotes aggregation or translocation of NADPH oxidase subunits and thereby form MR redox signaling platforms in ECs after death-receptor activation or upon stimulation of various endothelial injury factors including FasL, TNF-α, and endostatin (Zhang et al., 2006). In the present study, we demonstrated that OxLDL also induced the formation of large number of MR redox signaling platforms (characterized by $gp91^{phox}$ aggregation in and $p47^{phox}$ translocation into MR clusters) and consequent production of $O_2^{\cdot -}$ in ECs. These results support the view that the MRs clustering induced by OxLDL serves as a membrane platform for assembling of NADPH oxidase subunits to form an active enzyme complex. To our knowledge, our findings for the first time reveal the role of MR redox signaling platform associated with NADPH oxidase in OxLDL-induced $O_2^{\cdot -}$ production in coronary ECs. Targeting the formation of this MR redox signaling platform may be an important therapeutic strategy for improvement of endothelial function and prevention of atherosclerosis. The present study explores this possibility by using statins, a group of commonly used cholesterol-lowering compounds.

MRs are dynamic assemblies of cholesterol, lipids with saturated acyl chains, such as sphingolipids and glycosphingolipids. Given the fact that the integrity of MRs is highly dependent on the

Downloaded from jpet.aspetjournals.org at ASPET Journals on April 9, 2024

JPET Fast Forward. Published on February 22, 2013 as DOI: 10.1124/jpet.112.201442
This article has not been copyedited and formatted. The final version may differ from this version.

cholesterol level in the plasma membrane and several chemical cholesterol chelators including methyl-β-cyclodextrin and filipin are MR disruptors, MRs may serve as potential targets for the classical cholesterol inhibition action of statins. In the present study, we demonstrated that pravastatin and simvastatin markedly attenuated MR clustering induced by OxLDL in HCAECs and mevalonate indicating that mevalonate pathway-mediated cholesterol may be important for OxLDL-induced MR clustering. Moreover, MR-mediated $O_2^{-\cdot}$ production induced by OxLDL was also abolished by pravastatin and simvastatin in a similar action to the MR disruptors methyl-β-cyclodextrin and filipin, which deplete cholesterol in the plasma membrane. Thus, our results suggest that statins may inhibit MR clustering by decreasing cholesterol levels in ECs. In line with our view, a recent study has reported that statins (lovastatin and atorvastatin) disrupt MRs leading to decreased MR expression of lectin-like oxidized low-density lipoprotein (LOX-1), the primary receptor for OxLDL in ECs (Matarazzo et al., 2012). Further, cholesterol depletion but not inhibition of farnesylation mimicked the inhibitory effects as statins on the distribution and function of LOX-1 receptors strongly suggesting that the effect of statins on the LOX-1 receptor is related to statin-mediated cholesterol-lowering activity (Matarazzo et al., 2012). In the present study, we also demonstrated that farnesol but not geranylgerniol overcame the inhibitory effect of statins on MR clustering. Because farnesol restores both cholesterol synthesis and farnesylation, while geranylgerniol rescues the geranylgeranylation, our data together with previous findings suggest that statins may inhibit the formation of MR redox signaling platforms mainly depend on their cholesterol-lowering action preventing endothelial dysfunction in coronary arteries.

Previous studies have demonstrated that the formation of MR redox signaling platforms in the EC membrane is associated with ceramide production via lysosomal ASM, which is translocated onto the plasma membrane via membrane proximal lysosome trafficking and fusion upon stimulation (Jin et al., 2008b; Bao et al., 2010a; Bao et al., 2010b). Ceramides spontaneously fuse MRs into large ceramide-enriched membrane domains, which can serve as MR redox signaling platforms (Zhang et al., 2007; Zhang et al., 2009). In the present study, we found that statins blocked the translocation of ASM into and ceramide production in MR clusters induced by OxLDL. Our previous studies have demonstrated that ASM-ceramide signaling is essential for aggregating NADPH oxidase subunits in MR clusters and amplifies MR-NADPH oxidase-mediated redox signaling in ECs (Zhang et al.,

Downloaded from jpet.aspetjournals.org at ASPET Journals on April 9, 2024

JPET Fast Forward. Published on February 22, 2013 as DOI: 10.1124/jpet.112.201442
This article has not been copyedited and formatted. The final version may differ from this version.

2006; Zhang et al., 2007). The present study demonstrated that statins abolished OxLDL-induced aggregation of NADPH oxidase subunits $gp91^{phox}$ and $p47^{phox}$ in MR clusters. Thus, our data implicate that disruption of MR integrity by statins prevents ceramide-mediated MR clustering and the formation of ceramide-enriched platforms in the EC membrane. Such reduction of MR clustering further prevents the assembly of NADPH oxidase subunits in MR platforms and subsequent redox signaling pathway activated by OxLDL. Notably, cholesterol-lowering effect of statins contributes to decreased expression in caveolin-1, a structural protein of membrane caveolae, and thereby results in disruption of membrane caveolae (the flask-shape plasma membrane invaginations enriched in caveolin-1) (Ehrenstein et al., 2005; Jury and Ehrenstein, 2005). In this way, statins disrupt the inhibitory effect of caveolin-1 on eNOS activity, thereby increasing the bioavailability of nitric oxide (NO) which decreases $O_2^{\cdot-}$ level in ECs. Thus, these studies suggest that the cholesterol-lowering action of statins may have dual effects on inhibiting NADPH oxidase-derived redox signaling via direct disruption of MR redox signaling or by enhancing eNOS/NO signaling.

In addition, non-cholesterol lowering mechanisms by statins have also been attributed to inhibit NADPH oxidase associated redox signaling (Mason et al., 2004) (Hattori et al., 2003; Heeba et al., 2007). For example, statins block HMG-CoA reductase and the synthesis of isoprenoids and isoprenylation of Rac is essential for Rac translocation to plasma membrane and its activation. Activation of NADPH oxidase requires small GTPase Rac translocation to membrane to form integrated enzyme complex with other NADPH oxidase subunits (Van Aelst and D'Souza-Schorey, 1997; Hall, 1998; Liao and Laufs, 2005). In this regard, statin-inhibited NADPH oxidase activation has been attributed to their inhibitory effects on Rac. However, our data showed that overexpression of oncogenic Rac1 did not reverse the inhibitory effects of statins on OxLDL-induced MR clustering (Fig.1C) suggesting that Rac1 activation is insufficient to overcome the inhibitory effects of statins on the formation of MR redox signaling platforms. We further demonstrated that sphingomyelinase-induced $O_2^{\cdot-}$ production in HCAECs was abolished by pravastatin and simvastatin (Fig.4C), which further confirms that the disruption of ceramide-enriched MR redox signaling platforms by statins is independent of their inhibitory effect on Rac1 activity. Taken together, it seems that statins may have multiple effects on NADPH oxidase-derived redox signaling in ECs: statins may either directly inhibit the formation MR redox signaling platforms to disrupt NADPH

Downloaded from jpet.aspetjournals.org at ASPET Journals on April 9, 2024

JPET Fast Forward. Published on February 22, 2013 as DOI: 10.1124/jpet.112.201442
This article has not been copyedited and formatted. The final version may differ from this version.

oxidase assembly or inhibit Rac-mediated NADPH oxidase activation, or indirectly increase NO bioavailability by attenuation of caveolin-1-mediated eNOS inhibition. Nonetheless, the present study, for the first time, reveals a previous unidentified action of statins to inhibit NADPH oxidase activity via disrupting the formation of MR redox signaling platforms.

We also performed animal experiments *in vivo* to determine whether statins indeed prevent MRs clustering and consequent ROS production in the coronary arterial wall. We found that in the coronary arterial endothelium of mice with acute hypercholesterolemia MR clustering was indeed increased as shown by more patch staining of the arterial intima with fluorescent anti-flotill-1in antibody. The co-localization of this MR marker with NADPH oxidase subunits, $gp91^{phox}$ or $p47^{phox}$ was also detected. However, this patch staining of MR marker and co-localization with NADPH oxidase subunits were substantially blocked by pretreatment of mice with statins. In all groups of mice statins had no effect on mRNA levels of $gp91^{phox}$ or $p47^{phox}$ (**Supplementary Figure 1**) confirming that statins inhibit NADPH oxidase activation rather than gene expression. Furthermore, double staining of MR marker flotillin-1 with ASM or ceramide showed that hypercholesterolemic mice also exhibited enhanced formation of ceramide-enriched platforms in the intima of coronary arteries of hypercholesterolemic mice. In mice receiving statins, the formation of ceramide-enriched platforms was almost completely blocked. Moreover, our preliminary study demonstrated that P407 had no effect on MR clustering in HCAECs suggesting that MR clustering and formation of redox signaling platforms *in vivo* is associated with P407-induced cholesterol increase rather than direct interaction between P407 and MRs. Taken together, these results demonstrate that the ceramide-enriched MR redox signaling platforms associated with NADPH oxiase are increasingly formed in the intact arterial endothelium of hypercholesterolemic mice and that statins block the formation of this ceramide-enriched MR redox signaling platform.

The next question addressed in the present study was whether assembled NADPH oxidase in such MR redox signaling platforms is activated to produce $O_2^{\cdot -}$ in the coronary arterial endothelium in mice under hypercholesterolemia and whether satins interfere with NADPH oxidase activation *in vivo*. As measured by DHE fluorescence analysis, $O_2^{\cdot -}$ production was indeed increased in the coronary arteries from hypercholesterolemic mice compared to normal mice, which was attenuated

Downloaded from jpet.aspetjournals.org at ASPET Journals on April 9, 2024

JPET Fast Forward. Published on February 22, 2013 as DOI: 10.1124/jpet.112.201442
This article has not been copyedited and formatted. The final version may differ from this version.

by pretreatment of mice with statins. It is obvious that MR clustering-associated assembly of NADPH oxidase in the cell membrane leads to activation of this $O_2^{\cdot-}$-producing enzyme.

In summary, the present study demonstrated that acute treatment of coronary arterial ECs with statins inhibited OxLDL-induced MR clustering, ASM translocation into membrane, ceramide production and the formation of MR redox signaling platforms in these ECs *in vitro*. The inhibitory effect of statins on MR redox signaling is associated with their cholesterol-lowering action. In acute hypercholesterolemic mice, statins also abolished MR redox signaling and $O_2^{\cdot-}$ production in the coronary arterial wall. Our results for the first time identify that the direct inhibitory effects of statins on MR redox signaling associated with NADPH oxidase activation, which may contribute to the beneficial effects of statins in the protection of coronary arteries from endothelial dysfunction, inflammatory injury, and ultimate atherosclerosis.

Disclosures

None

Authorship Contributions

Participated in research design: Wei, P.-L. Li, and Zhang.

Conducted experiments: Wei, X. Li, J.X., Xia, Abais, Boini and Zhang.

Performed data analysis: Wei, X. Li and Zhang.

Wrote or contributed to the writing of the manuscript: Wei, X. Li, P.-L.Li, and Zhang.

Downloaded from jpet.aspetjournals.org at ASPET Journals on April 9, 2024

JPET Fast Forward. Published on February 22, 2013 as DOI: 10.1124/jpet.112.201442
This article has not been copyedited and formatted. The final version may differ from this version.

Reference

(1994) Randomised trial of cholesterol lowering in 4444 patients with coronary heart disease: the Scandinavian Simvastatin Survival Study (4S). *Lancet* **344**:1383-1389.

(1998) Prevention of cardiovascular events and death with pravastatin in patients with coronary heart disease and a broad range of initial cholesterol levels. The Long-Term Intervention with Pravastatin in Ischaemic Disease (LIPID) Study Group. *N Engl J Med* **339**:1349-1357.

Alvarez E, Rodino-Janeiro BK, Ucieda-Somoza R and Gonzalez-Juanatey JR (2010) Pravastatin counteracts angiotensin II-induced upregulation and activation of NADPH oxidase at plasma membrane of human endothelial cells. *J Cardiovasc Pharmacol* **55**:203-212.

Araki K, Masaki T, Katsuragi I, Kakuma T and Yoshimatsu H (2008) Effects of pravastatin on obesity, diabetes, and adiponectin in diet-induced obese mice. *Obesity (Silver Spring)* **16**:2068-2073.

Bao JX, Jin S, Zhang F, Wang ZC, Li N and Li PL (2010a) Activation of membrane NADPH oxidase associated with lysosome-targeted acid sphingomyelinase in coronary endothelial cells. *Antioxid Redox Signal* **12**:703-712.

Bao JX, Xia M, Poklis JL, Han WQ, Brimson C and Li PL (2010b) Triggering role of acid sphingomyelinase in endothelial lysosome-membrane fusion and dysfunction in coronary arteries. *Am J Physiol Heart Circ Physiol* **298**:H992-H1002.

Bao XM, Wu CF and Lu GP (2010c) Atorvastatin inhibits homocysteine-induced dysfunction and apoptosis in endothelial progenitor cells. *Acta Pharmacol Sin* **31**:476-484.

Bea F, Blessing E, Bennett B, Levitz M, Wallace EP and Rosenfeld ME (2002) Simvastatin promotes atherosclerotic plaque stability in apoE-deficient mice independently of lipid lowering. *Arterioscler Thromb Vasc Biol* **22**:1832-1837.

Briones AM, Rodriguez-Criado N, Hernanz R, Garcia-Redondo AB, Rodrigues-Diez RR, Alonso MJ, Egido J, Ruiz-Ortega M and Salaices M (2009) Atorvastatin prevents angiotensin II-induced vascular remodeling and oxidative stress. *Hypertension* **54**:142-149.

Bu DX, Griffin G and Lichtman AH (2011) Mechanisms for the anti-inflammatory effects of statins. *Curr Opin Lipidol* **22**:165-170.

Chow SE, Hshu YC, Wang JS and Chen JK (2007) Resveratrol attenuates oxLDL-stimulated NADPH oxidase activity and protects endothelial cells from oxidative functional damages. *J Appl Physiol* **102**:1520-1527.

Dje N'Guessan P, Riediger F, Vardarova K, Scharf S, Eitel J, Opitz B, Slevogt H, Weichert W, Hocke AC, Schmeck B, Suttorp N and Hippenstiel S (2009) Statins control oxidized LDL-mediated histone modifications and gene expression in cultured human endothelial cells. *Arterioscler Thromb Vasc Biol* **29**:380-386.

Ehrenstein MR, Jury EC and Mauri C (2005) Statins for atherosclerosis--as good as it gets? *N Engl J Med* **352**:73-75.

Gerson RJ, MacDonald JS, Alberts AW, Kornbrust DJ, Majka JA, Stubbs RJ and Bokelman DL (1989) Animal safety and toxicology of simvastatin and related hydroxy-methylglutaryl-coenzyme A reductase inhibitors. *Am J Med* **87**:28S-38S.

Greenwood J and Mason JC (2007) Statins and the vascular endothelial inflammatory response. *Trends Immunol* **28**:88-98.

Hall A (1998) Rho GTPases and the actin cytoskeleton. *Science* **279**:509-514.

Hattori Y, Nakanishi N, Akimoto K, Yoshida M and Kasai K (2003) HMG-CoA reductase inhibitor

Downloaded from jpet.aspetjournals.org at ASPET Journals on April 9, 2024

JPET Fast Forward. Published on February 22, 2013 as DOI: 10.1124/jpet.112.201442
This article has not been copyedited and formatted. The final version may differ from this version.

increases GTP cyclohydrolase I mRNA and tetrahydrobiopterin in vascular endothelial cells. *Arterioscler Thromb Vasc Biol* **23**:176-182.

Heeba G, Hassan MK, Khalifa M and Malinski T (2007) Adverse balance of nitric oxide/peroxynitrite in the dysfunctional endothelium can be reversed by statins. *J Cardiovasc Pharmacol* **50**:391-398.

Heinecke JW (2006) Lipoprotein oxidation in cardiovascular disease: chief culprit or innocent bystander? *J Exp Med* **203**:813-816.

Jacobson JR (2009) Statins in endothelial signaling and activation. *Antioxid Redox Signal* **11**:811-821.

Jankov RP, Kantores C, Belcastro R, Yi S, Ridsdale RA, Post M and Tanswell AK (2005) A role for platelet-derived growth factor beta-receptor in a newborn rat model of endothelin-mediated pulmonary vascular remodeling. *Am J Physiol Lung Cell Mol Physiol* **288**:L1162-1170.

Jankov RP, Kantores C, Pan J and Belik J (2008) Contribution of xanthine oxidase-derived superoxide to chronic hypoxic pulmonary hypertension in neonatal rats. *Am J Physiol Lung Cell Mol Physiol* **294**:L233-245.

Jin S, Yi F, Zhang F, Poklis JL and Li PL (2008a) Lysosomal targeting and trafficking of acid sphingomyelinase to lipid raft platforms in coronary endothelial cells. *Arterioscler Thromb Vasc Biol* **28**:2056-2062.

Jin S, Zhang Y, Yi F and Li PL (2008b) Critical role of lipid raft redox signaling platforms in endostatin-induced coronary endothelial dysfunction. *Arteriosclerosis, thrombosis, and vascular biology* **28**:485-490.

Johnston TP, Jaye M, Webb CL, Krawiec JA, Alom-Ruiz SP, Sachs-Barrable K and Wasan KM (2006) Poloxamer 407 (P-407)-mediated reduction in the gene expression of ATP-binding-cassette transporter A1 may contribute to increased cholesterol in peripheral tissues of P-407-treated rats. *Eur J Pharmacol* **536**:232-240.

Jury EC and Ehrenstein MR (2005) Statins: immunomodulators for autoimmune rheumatic disease? *Lupus* **14**:192-196.

Li D and Mehta JL (2005) Oxidized LDL, a critical factor in atherogenesis. *Cardiovasc Res* **68**:353-354.

Liao JK and Laufs U (2005) Pleiotropic effects of statins. *Annu Rev Pharmacol Toxicol* **45**:89-118.

Libby P, Ridker PM and Hansson GK (2009) Inflammation in atherosclerosis: from pathophysiology to practice. *J Am Coll Cardiol* **54**:2129-2138.

Mason RP, Walter MF and Jacob RF (2004) Effects of HMG-CoA reductase inhibitors on endothelial function: role of microdomains and oxidative stress. *Circulation* **109**:II34-41.

Matarazzo S, Quitadamo MC, Mango R, Ciccone S, Novelli G and Biocca S (2012) Cholesterol-lowering drugs inhibit lectin-like oxidized low-density lipoprotein-1 receptor function by membrane raft disruption. *Mol Pharmacol* **82**:246-254.

Natoli G, Costanzo A, Guido F, Moretti F and Levrero M (1998) Apoptotic, non-apoptotic, and anti-apoptotic pathways of tumor necrosis factor signalling. *Biochem Pharmacol* **56**:915-920.

Nijmeh J, Moldobaeva A and Wagner EM (2010) Role of ROS in ischemia-induced lung angiogenesis. *Am J Physiol Lung Cell Mol Physiol* **299**:L535-541.

Pepys MB, Hirschfield GM, Tennent GA, Gallimore JR, Kahan MC, Bellotti V, Hawkins PN, Myers RM, Smith MD, Polara A, Cobb AJ, Ley SV, Aquilina JA, Robinson CV, Sharif I, Gray GA, Sabin CA, Jenvey MC, Kolstoe SE, Thompson D and Wood SP (2006) Targeting C-reactive

Downloaded from jpet.aspetjournals.org at ASPET Journals on April 9, 2024

JPET Fast Forward. Published on February 22, 2013 as DOI: 10.1124/jpet.112.201442
This article has not been copyedited and formatted. The final version may differ from this version.

protein for the treatment of cardiovascular disease. *Nature* **440**:1217-1221.

Ridker PM, Danielson E, Fonseca FA, Genest J, Gotto AM, Jr., Kastelein JJ, Koenig W, Libby P, Lorenzatti AJ, MacFadyen JG, Nordestgaard BG, Shepherd J, Willerson JT and Glynn RJ (2008) Rosuvastatin to prevent vascular events in men and women with elevated C-reactive protein. *N Engl J Med* **359**:2195-2207.

Sharyo S, Yokota-Ikeda N, Mori M, Kumagai K, Uchida K, Ito K, Burne-Taney MJ, Rabb H and Ikeda M (2008) Pravastatin improves renal ischemia-reperfusion injury by inhibiting the mevalonate pathway. *Kidney Int* **74**:577-584.

Steinberg D and Witztum JL (2002) Is the oxidative modification hypothesis relevant to human atherosclerosis? Do the antioxidant trials conducted to date refute the hypothesis? *Circulation* **105**:2107-2111.

Tawfik HE, El-Remessy AB, Matragoon S, Ma G, Caldwell RB and Caldwell RW (2006) Simvastatin improves diabetes-induced coronary endothelial dysfunction. *J Pharmacol Exp Ther* **319**:386-395.

Van Aelst L and D'Souza-Schorey C (1997) Rho GTPases and signaling networks. *Genes Dev* **11**:2295-2322.

Vecchione C, Gentile MT, Aretini A, Marino G, Poulet R, Maffei A, Passarelli F, Landolfi A, Vasta A and Lembo G (2007) A novel mechanism of action for statins against diabetes-induced oxidative stress. *Diabetologia* **50**:874-880.

Wagner AH, Kohler T, Ruckschloss U, Just I and Hecker M (2000) Improvement of nitric oxide-dependent vasodilatation by HMG-CoA reductase inhibitors through attenuation of endothelial superoxide anion formation. *Arterioscler Thromb Vasc Biol* **20**:61-69.

Wang CY, Liu PY and Liao JK (2008) Pleiotropic effects of statin therapy: molecular mechanisms and clinical results. *Trends Mol Med* **14**:37-44.

Yi F, Xia M, Li N, Zhang C, Tang L and Li PL (2009) Contribution of guanine nucleotide exchange factor Vav2 to hyperhomocysteinemic glomerulosclerosis in rats. *Hypertension* **53**:90-96.

Zhang AY, Yi F, Jin S, Xia M, Chen QZ, Gulbins E and Li PL (2007) Acid sphingomyelinase and its redox amplification in formation of lipid raft redox signaling platforms in endothelial cells. *Antioxid Redox Signal* **9**:817-828.

Zhang AY, Yi F, Zhang G, Gulbins E and Li PL (2006) Lipid raft clustering and redox signaling platform formation in coronary arterial endothelial cells. *Hypertension* **47**:74-80.

Zhang DX, Yi FX, Zou AP and Li PL (2002) Role of ceramide in TNF-alpha-induced impairment of endothelium-dependent vasorelaxation in coronary arteries. *Am J Physiol Heart Circ Physiol* **283**:H1785-1794.

Zhang Y, Li X, Becker KA and Gulbins E (2009) Ceramide-enriched membrane domains--structure and function. *Biochim Biophys Acta* **1788**:178-183.

Zhu Y, Liao H, Xie X, Yuan Y, Lee TS, Wang N, Wang X, Shyy JY and Stemerman MB (2005) Oxidized LDL downregulates ATP-binding cassette transporter-1 in human vascular endothelial cells via inhibiting liver X receptor (LXR). *Cardiovasc Res* **68**:425-432.

Downloaded from jpet.aspetjournals.org at ASPET Journals on April 9, 2024

JPET Fast Forward. Published on February 22, 2013 as DOI: 10.1124/jpet.112.201442
This article has not been copyedited and formatted. The final version may differ from this version.

Footnote

This study was supported by grants from the National Institute of Health (HL057244, HL075316, and HL091464); Y.Z. shares the corresponding authorship with P.-L.Li.

Downloaded from jpet.aspetjournals.org at ASPET Journals on April 9, 2024

JPET Fast Forward. Published on February 22, 2013 as DOI: 10.1124/jpet.112.201442
This article has not been copyedited and formatted. The final version may differ from this version.

Figure Legends

Fig. 1. OxLDL-induced MR clustering in HCAECs in the absence or presence of statins. HCAECs were stimulated with control, OxLDL (100 μg/mL, 30 min) without or with pravastatin (Prava, 10 μM)/simvastatin (Simva, 5 μM) pretreatment and stained with a MR probe, Alexa 488-cholera toxin B (Al488-CTXB). (**A**) Representative images of HCAECs with Al488-CTXB staining. (**B**) Summarized dose effects of OxLDL (25-150 μg/mL, 30 min) on the MR clustering as indicated by percentage of positive cells with CTXB staining (n = 4). (**C**) Summarized effects of statins on OxLDL-induced MR clustering (n = 4). Some groups of cells were pretreated with mevalonate (Mev, 10 μM), farnesol (Far, 10 μM), geranylgeraniol (Ger, 10 μM), or transfected with oncogenic Rac1 cDNA. Shown is the percentage of cells with MR clustering. * P<0.05 *vs.* control; # P<0.05 *vs.* vehicle; $ P<0.05 *vs*. statin.

Fig. 2. Effects of statins on OxLDL-induced co-localization of ASM and ceramide in HCAECs. Cells were stained with Alexa488-conjugated anti-ASM and Texas Red (TR)-conjugated anti-ceramide antibodies. (**A**) Representative images showed the co-localization (yellow) of ASM (green, Alexa488-anti-ASM) and ceramide (red, TR-anti-ceramide) under the stimulation of OxLDL (100 μg/mL) with or without pre-treatment of statins. (**B**) Summarized data show the co-localization co-efficiency indicating the relative ratio of cells with co-localized yellow spots (n = 5). *p<0.05 *vs.* control, # p<0.05 *vs.* vehicle.

Fig. 3. Effects of statins on OxLDL-induced co-localization of MR clusters and gp91^{phox} or p47^{phox} in HCAECs. Cells were stained with MR marker, Alexa488-CTXB and Texas red-conjugated anti-gp91^{phox} (TR-anti-gp91) or p47^{phox} (TR-anti-p47) antibody. Representative images showed the co-localization (yellow) of MR marker CTXB (green, Alexa488-CTXB) and gp91^{phox} (red, TR-anti-gp91) (A) or p47 (red, TR-anti-p47) (B) under the stimulation of OxLDL (100 μg/mL, 30 min) with or without pre-treatment of statins. (C) Summarized data show the co-localization co-efficiency indicating the relative ratio of cells with co-localized yellow spots (n = 5). * P<0.05 *vs*. control, # P<0.05 *vs.* vehicle.

Fig. 4. Electron spin resonance (ESR) spectrometric analysis of $O_2^{\cdot-}$ production in HCAECs

Downloaded from jpet.aspetjournals.org at ASPET Journals on April 9, 2024

JPET Fast Forward. Published on February 22, 2013 as DOI: 10.1124/jpet.112.201442
This article has not been copyedited and formatted. The final version may differ from this version.

stimulated by OxLDL in the absence or presence of statins. (A) Cells were pretreated with vehicle (Vehl), pravastatin (Prava, 10 μM) or simvastatin (Simva, 5 μM) and stimulated with OxLDL. Representative ESR spectrographs of $O_2^{\cdot -}$ trapped by 1-hydroxy-3-methoxycarbonyl-2,2,5,5-tetramethylpyrorolidine (CMH) with NADPH as substrates. (B) Summarized data show relative $O_2^{\cdot -}$ production induced by OxLDL compared to control (n = 5). (C) Summarized data show relative $O_2^{\cdot -}$ production induced by sphingomyelinase (SMase) compared to control (n = 5). Some groups of cells were pretreated with MR disruptors: methyl-β-cyclodextrin (MCD) or filipin. * P<0.05 *vs.* control; # P<0.05 *vs.* vehicle.

Fig. 5. Effect of statins on plasma cholesterol levels in mice with acute hypercholesterolemia. Mice were injected intraperitoneally with vehicle (Control) or poloxamer 407 (P407, 0.5 g/kg) to induce acute hypercholesterolemia (P407). In case of pretreatment with statins, mice were intragastric fed statins (pravastatin, 140 mg/kg per day; simvastatin, 70 mg/kg/d) for a week and then treated with vehicle (Statin) or P407 (Statin+P407). Summarized data show the plasma cholesterol concentrations in mice (n = 5). ** P<0.01 *vs.* control; ## P<0.01 *vs.* P407.

Fig 6. Statins block the NADPH oxidase subunits clustering in MR clusters in coronary arteries of mice with acute hypercholesterolemia. Frozen sections of mouse hearts were stained with Al488-anti-flotillin-1 and TR-anti $gp91^{phox}$ or TR-anti-$p47^{phox}$. Representative merged images displayed yellow dots or patches indicating the co-localization of MR marker protein flotillin-1 with NADPH oxidase subunit $gp91^{phox}$ (A) or $p47^{phox}$ (B). Each image includes an enlarged view of ROI (region of interest) at the lower right corner. Scale bar, 50 μm. (C) Summarized data show the co-localization co-efficiency (n = 5). * P<0.05 vs. control; # P<0.05 *vs.* vehicle.

Fig. 7. Statins block ceramide or ASM clustering in MR clusters in coronary arteries of mice with acute hypercholesterolemia. Frozen sections of mouse hearts were stained with Al488-anti-flotillin-1 and TR-anti-ASM or TR-anti-ceramide. Representative merged images displayed yellow dots or patches indicating the co-localization of MR marker protein flotillin-1 with ASM (A) or ceramide (B). Each image includes an enlarged view of ROI (region of interest) at the lower right corner. Scale bar, 50 μm. (C) Summarized data show the co-localization co-efficiency (n

Downloaded from jpet.aspetjournals.org at ASPET Journals on April 9, 2024

JPET Fast Forward. Published on February 22, 2013 as DOI: 10.1124/jpet.112.201442
This article has not been copyedited and formatted. The final version may differ from this version.

= 5). * P<0.05 vs. control; # P<0.05 *vs.* vehicle.

Fig. 8. Measurement of $O_2^{\cdot-}$ production *in situ* in mouse coronary arteries. (A) Frozen sections of hearts without fixation were incubated with DHE. Representative merged images (DHE red fluorescence merged with transmission light) show increases in DHE-$O_2^{\cdot-}$ fluorescence *in situ* in mouse coronary arteries. Scale bar, 50 μm. (B) Summarized data show the DHE fluorescence intensity (n = 5). ** P<0.01 *vs.* control; ## P<0.01 *vs.* vehicle.

Downloaded from jpet.aspetjournals.org at ASPET Journals on April 9, 2024

JPET Fast Forward. Published on February 27, 2013 as DOI: 10.1124/jpet.112.201442
This article has not been copyedited and formatted. The final version may differ from this version.

Figure 1

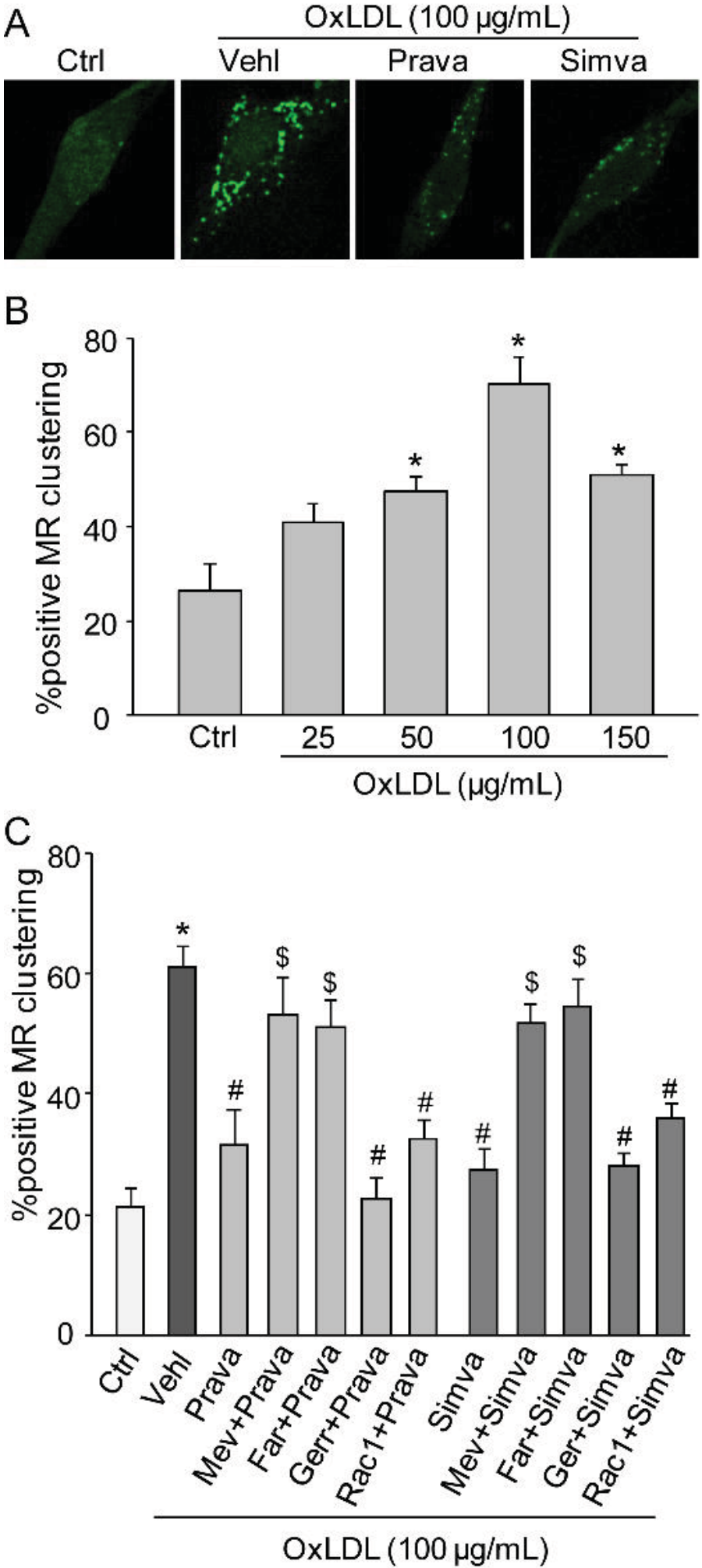

Downloaded from jpet.aspetjournals.org at ASPET Journals on April 9, 2024

JPET Fast Forward. Published on February 22, 2013 as DOI: 10.1124/jpet.112.201442
This article has not been copyedited and formatted. The final version may differ from this version.

Figure 2

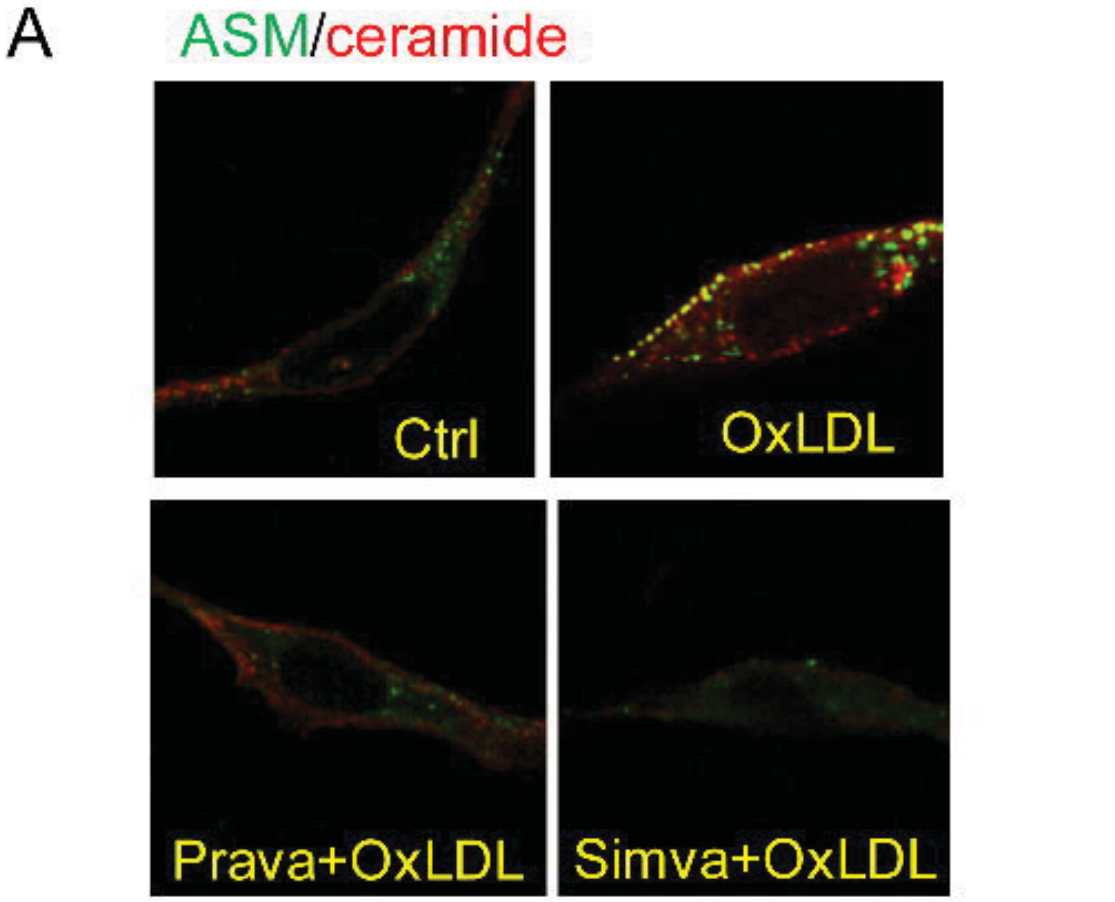

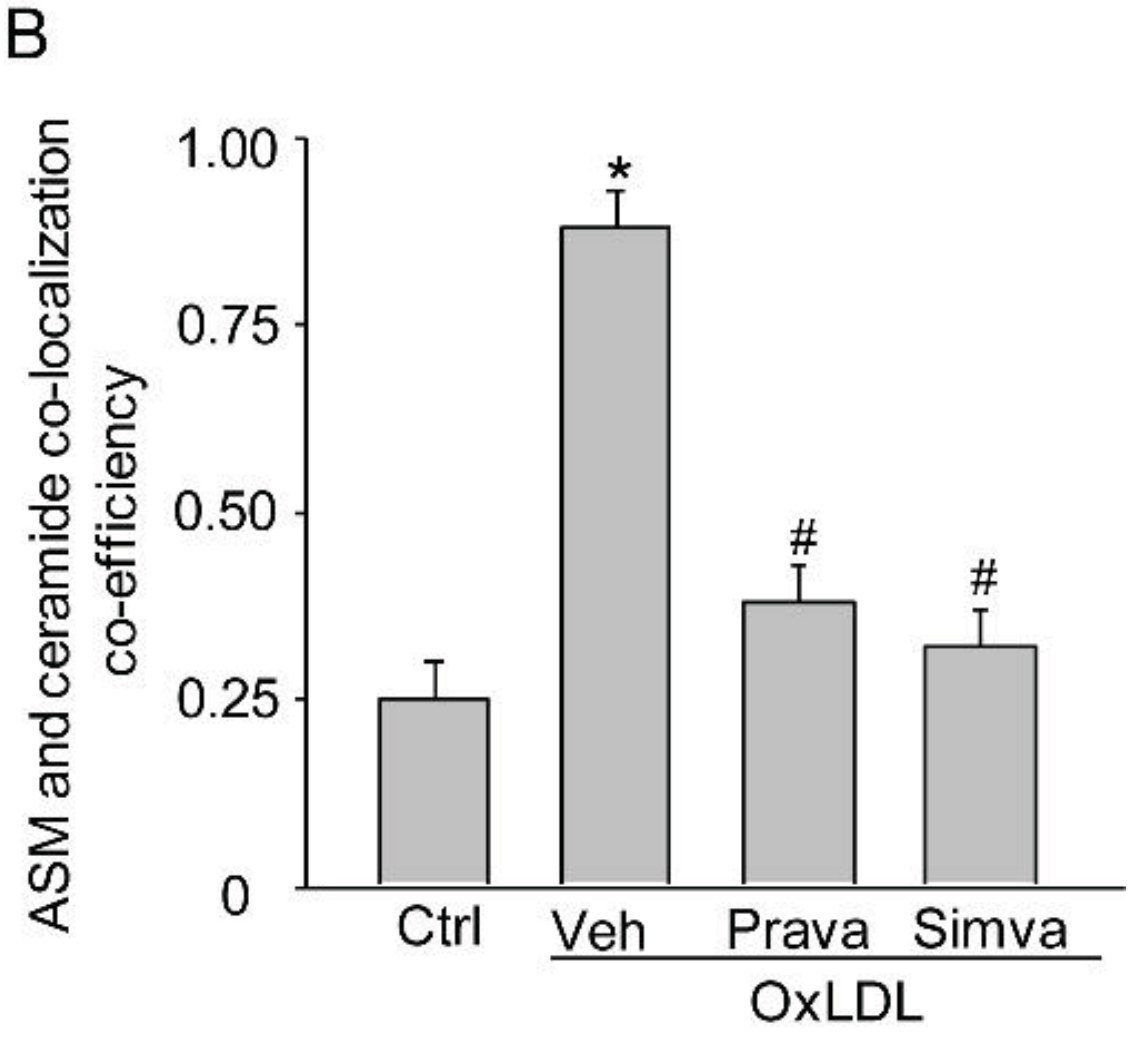

Downloaded from jpet.aspetjournals.org at ASPET Journals on April 9, 2024

JPET Fast Forward. Published on February 22, 2013 as DOI: 10.1124/jpet.112.201442
This article has not been copyedited and formatted. The final version may differ from this version.

Figure 3

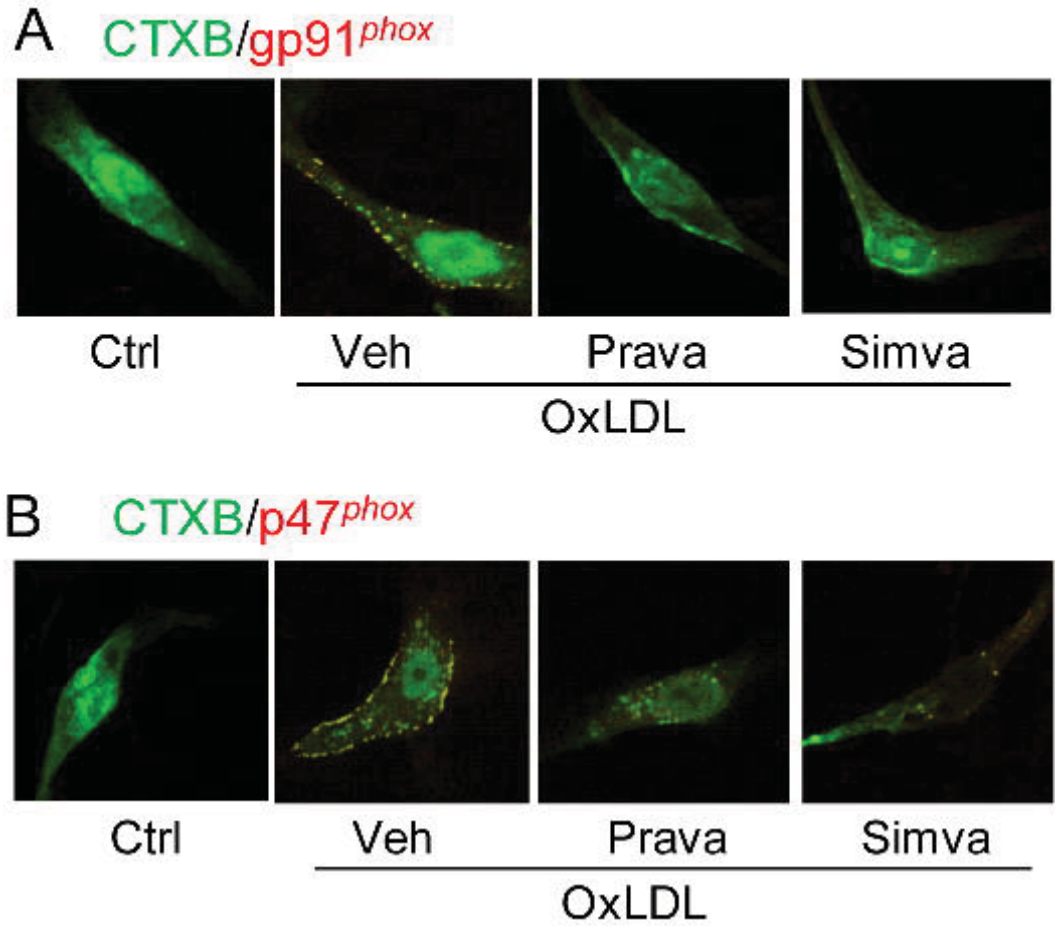

Downloaded from jpet.aspetjournals.org at ASPET Journals on April 9, 2024

JPET Fast Forward. Published on February 21, 2013 as DOI: 10.1124/jpet.112.201442
This article has not been copyedited and formatted. The final version may differ from this version.

Figure 4

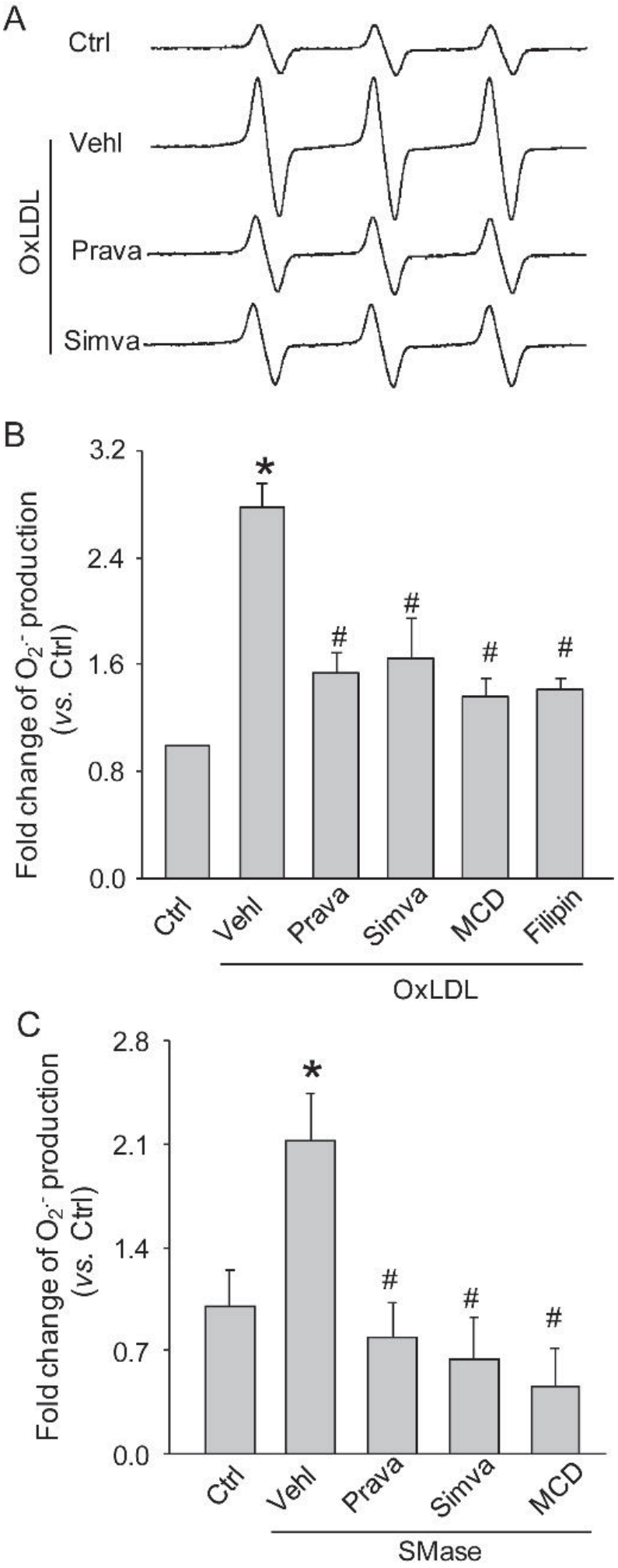

Downloaded from jpet.aspetjournals.org at ASPET Journals on April 9, 2024

JPET Fast Forward. Published on February 22, 2013 as DOI: 10.1124/jpet.112.201442
This article has not been copyedited and formatted. The final version may differ from this version.

Figure 5

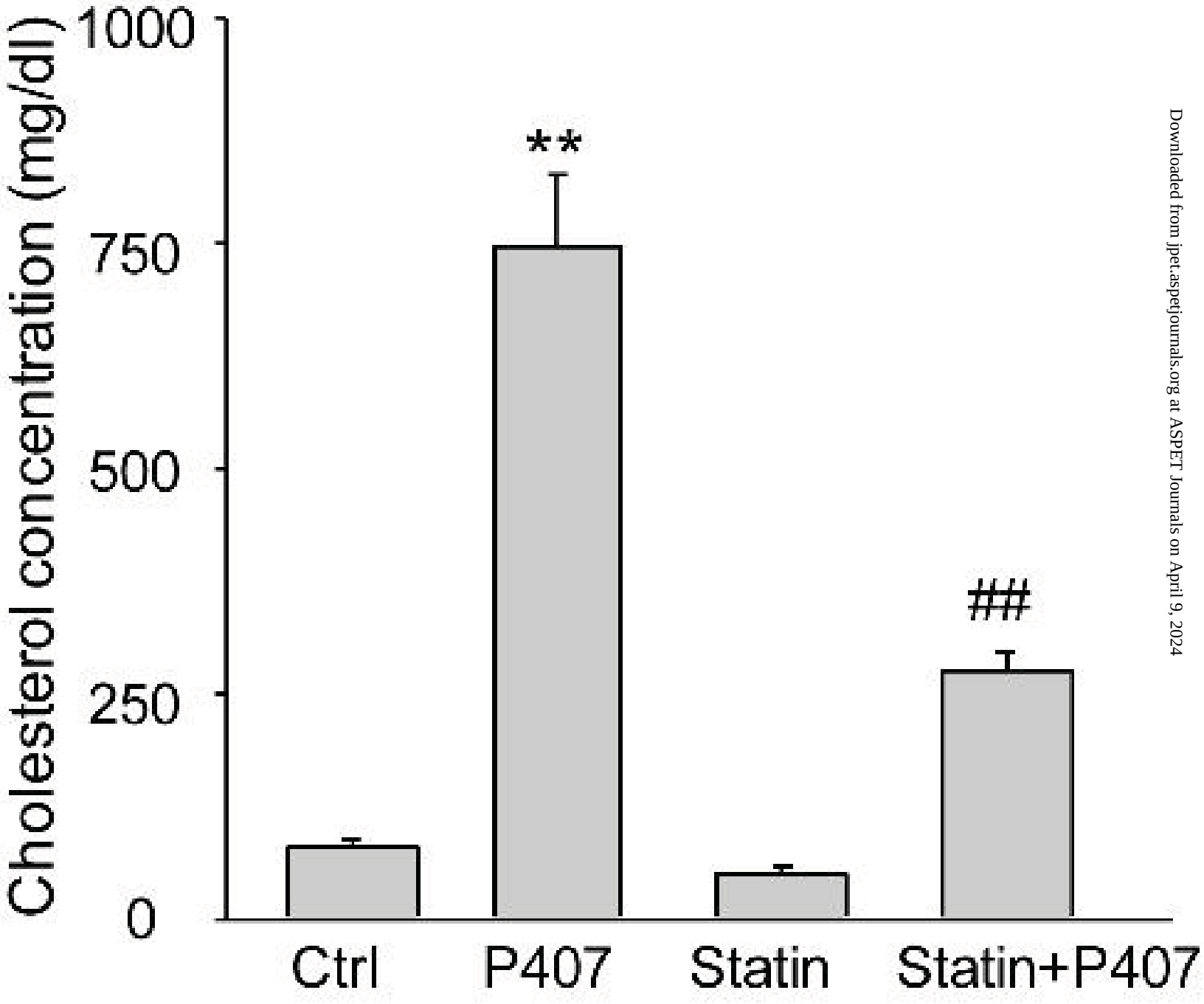

Downloaded from jpet.aspetjournals.org at ASPET Journals on April 9, 2024

JPET Fast Forward. Published on February 22, 2012 as DOI: 10.1124/jpet.112.201442
This article has not been copyedited and formatted. The final version may differ from this version.

Figure 6

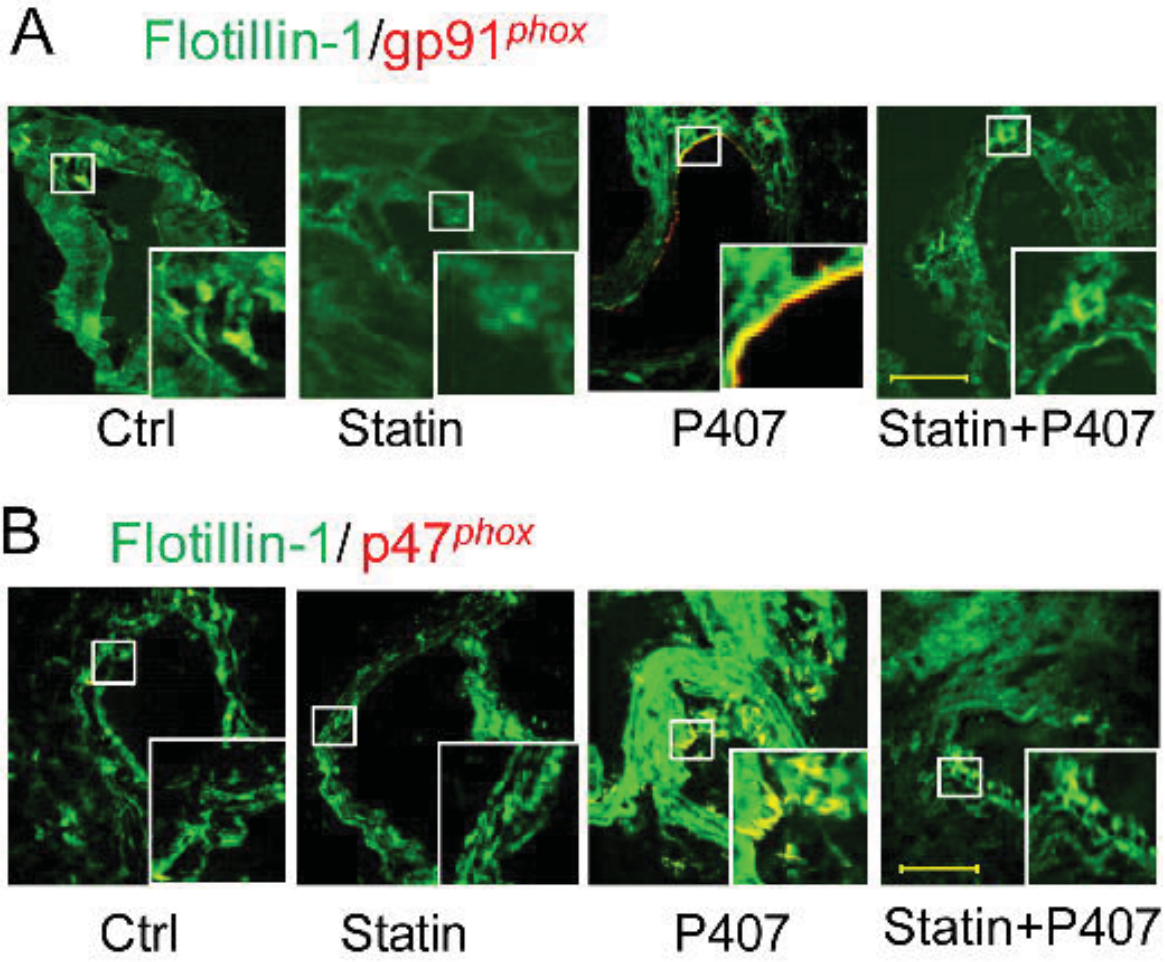

Downloaded from jpet.aspetjournals.org at ASPET Journals on April 9, 2024

JPET Fast Forward. Published on January 23, 2013 as DOI: 10.1124/jpet.112.201442
This article has not been copyedited and formatted. The final version may differ from this version.

Figure 7

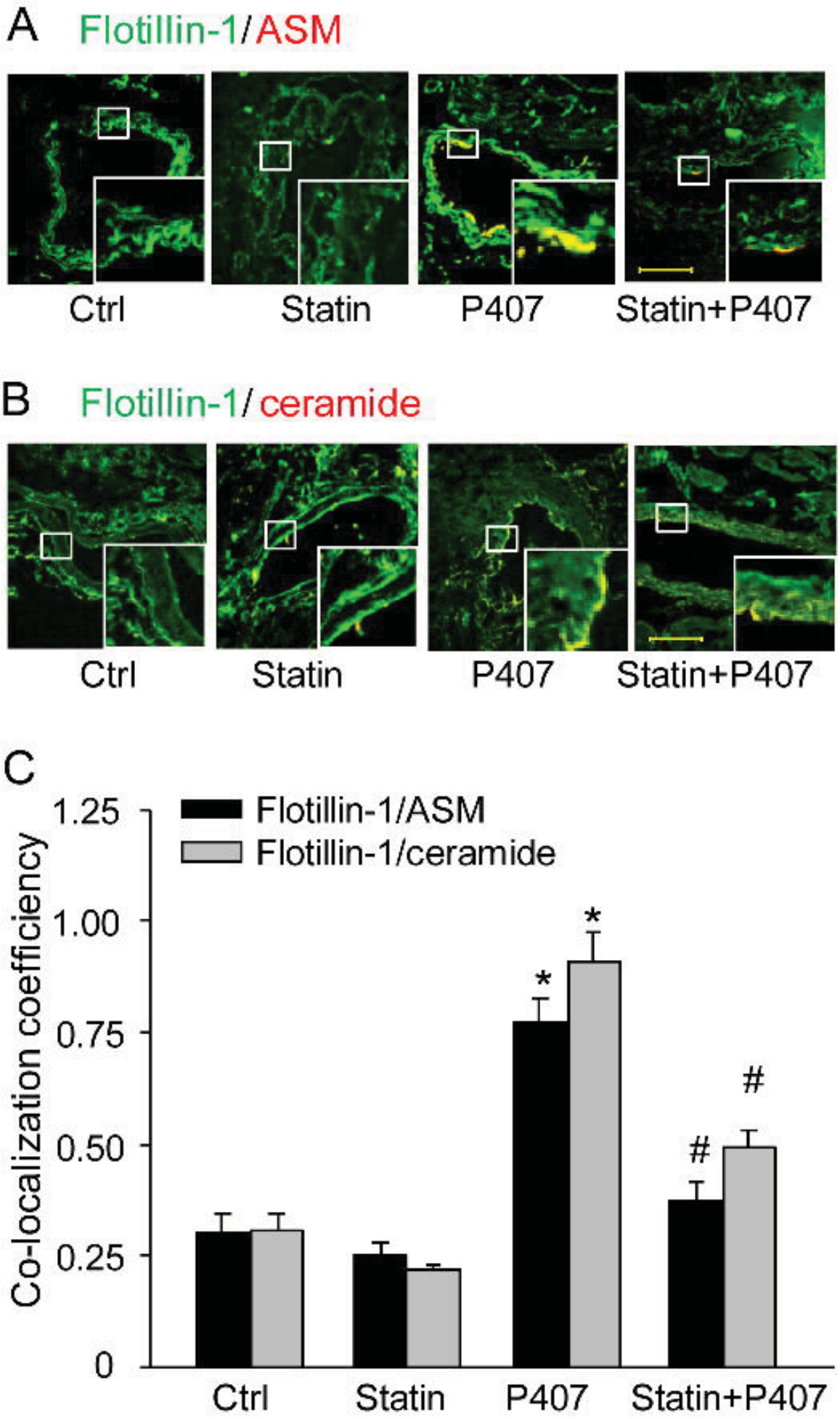

Downloaded from jpet.aspetjournals.org at ASPET Journals on April 9, 2024

JPET Fast Forward. Published on February 23, 2012 as DOI: 10.1124/jpet.112.201442
This article has not been copyedited and formatted. The final version may differ from this version.

Figure 8

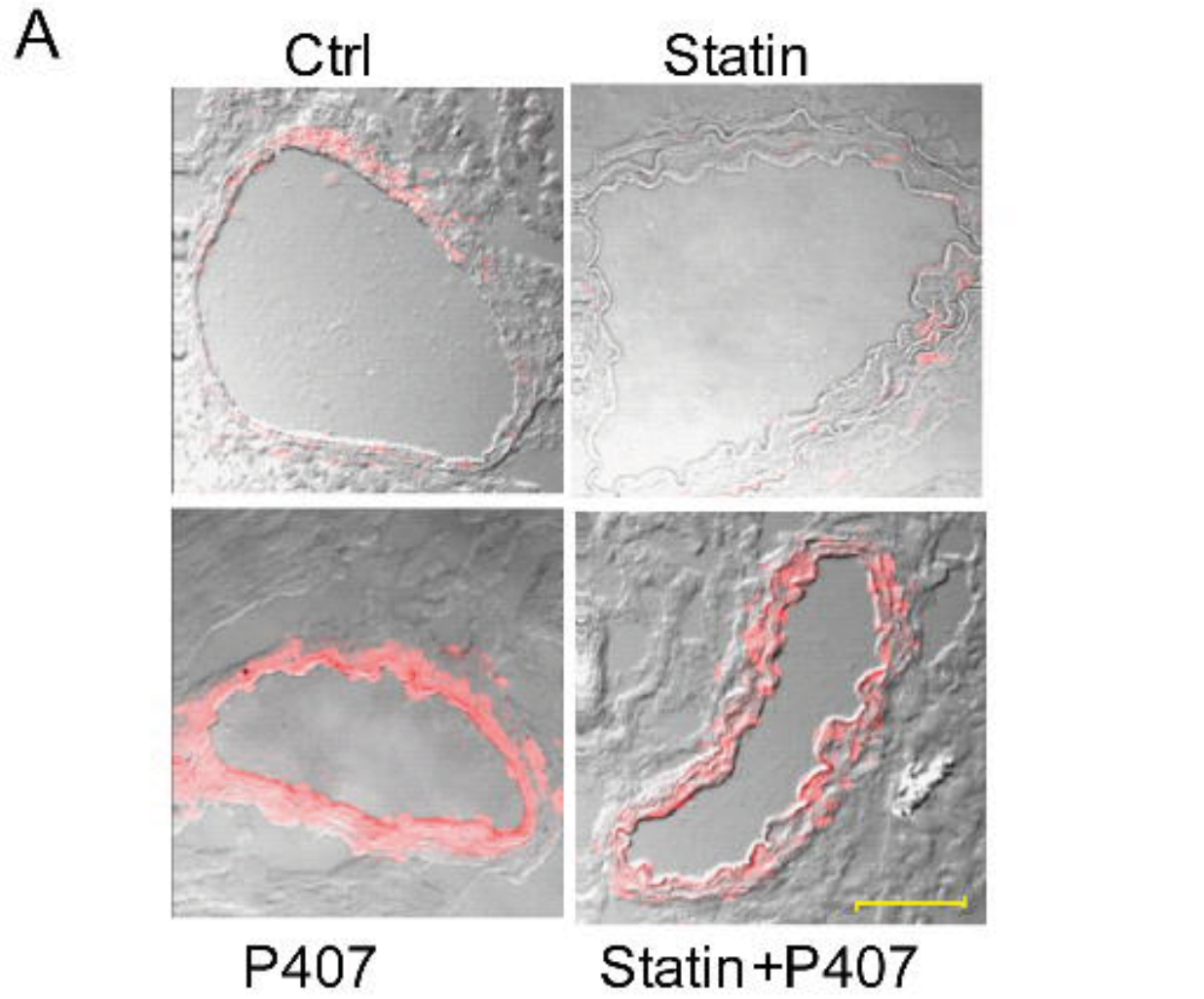

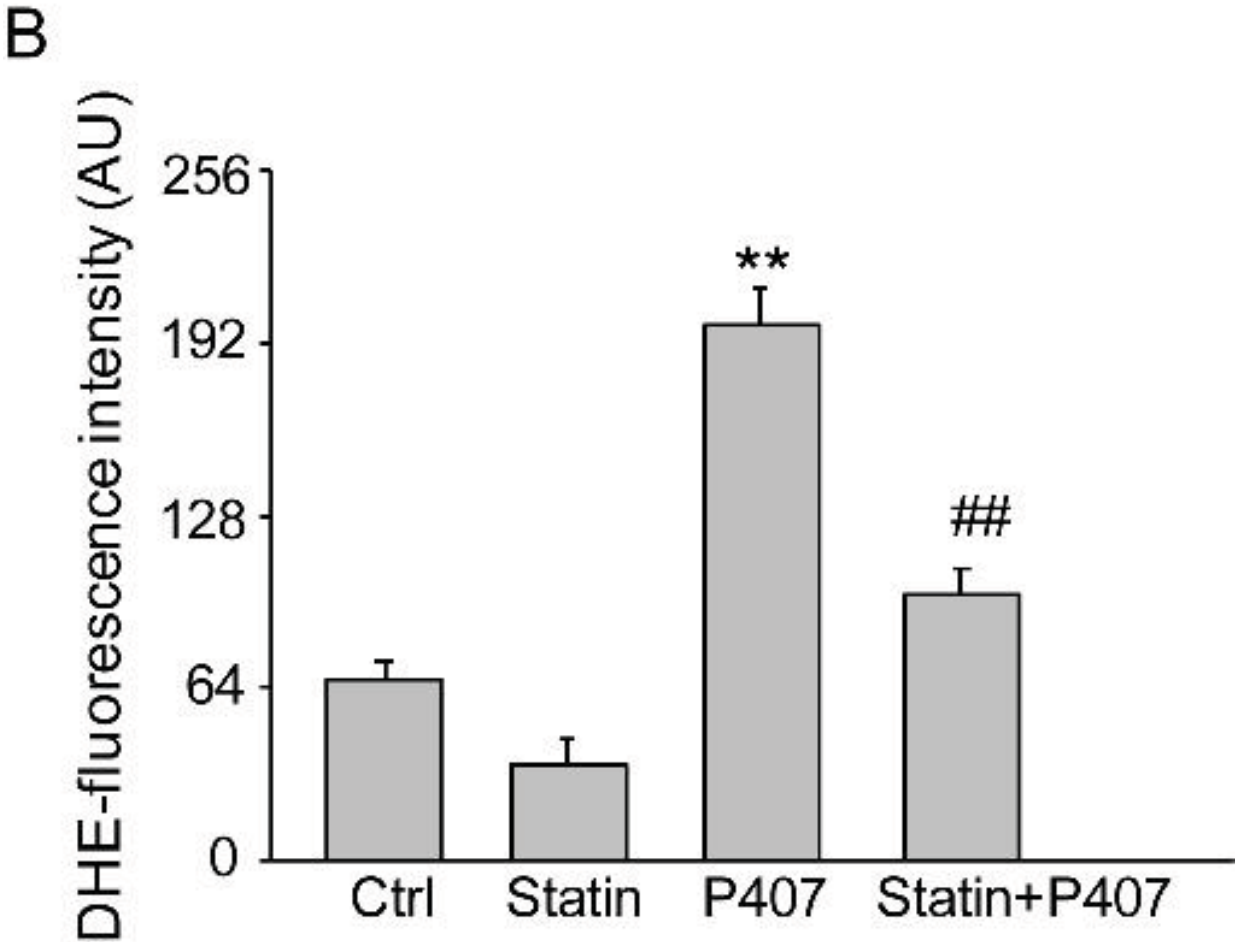

Downloaded from jpet.aspetjournals.org at ASPET Journals on April 9, 2024